Available online at http://scik.org
Commun. Math. Biol. Neurosci. 2025, 2025:55
https://doi.org/10.28919/cmbn/8987
ISSN: 2052-2541

ANALYSIS OF THE STABILITY OF A MATHEMATICAL MODEL FOR MEASLES

HICHAM GOURRAM[1,*], ISSAM SAHIB[1], MOHAMED BAROUDI[1], IMANE SMOUNI[1], ABDERRAHIM LABZAI[2], MOHAMED BELAM[1]

[1]Laboratory LMACS, Sultan Moulay Slimane University, MATIC Research Team: Applied Mathematics and Information and Communication Technologie, Department of Mathematics and Computer Science, Khouribga Polydisciplinary Faculty, Morocco

[2]Laboratory of Analysis Modeling and Simulation, Department of Mathematics and Computer Science, Faculty of Sciences Ben M'sik, Hassan II University of Casablanca, Morocco

Abstract. The worldwide measles crisis has escalated into a significant public health issue due to its lethal nature, generating widespread anxiety. Our study presents a dynamic mathematical model constructed using comprehensive mortality data from the World Health Organization and actual data on measles outbreak propagation. By utilizing the Routh-Hurwitz criteria and formulating Lyapunov functions, we demonstrated both local and global stability for scenarios with and without the presence of the disease. Furthermore, we conducted a sensitivity analysis on the model's parameters to assess their impact on the basic reproduction number, R_0. Our theoretical results were substantiated through numerical simulations performed with MATLAB.

Keywords: optimal control; measles; spread of infectious diseases.

2020 AMS Subject Classification: 93A30.

*Corresponding author

E-mail address: gourramhicham03@gmail.com

Received October 28, 2024

1. INTRODUCTION

Measles is an exceptionally contagious and serious disease triggered by the measles virus. It spreads through sneezing, coughing, and close contact with an infected person or their secretions. Symptoms typically appear $10-12$ days after exposure. Routine vaccination is the primary method for preventing measles in children. Historically, measles was one of the deadliest diseases globally. Before widespread vaccination began in 1963, the US reported about 500 deaths annually [1]. During $1989-1991$, over $55,000$ cases were reported. The introduction of the measles vaccine in 1989 significantly reduced the incidence of the disease, with some countries reporting fewer than 200 cases annually by 1997 [2]. However, the World Health Organization reported a significant increase in measles cases in 2012, particularly in developing countries with low vaccination rates, leading to $122,000$ deaths worldwide [3–8].

To effectively combat measles, it is crucial to model its transmission dynamics and study the impact of vaccination and quarantine measures. Mathematical modeling has become a valuable tool in understanding the spread of infectious diseases and developing strategies to control them [9–12]. Various studies have used these models to analyze the spread of the measles virus, evaluate the effectiveness of vaccines, and propose measures to curb its transmission. One study found that voluntary vaccination alone would not achieve optimal group immunity [13]. Recent developments in mathematical models have focused on the dynamics of disease transmission in different regions, providing insights into better prevention strategies [14–19].

Despite significant advancements, there remain substantial gaps in research regarding the integration of vaccination strategies with other public health measures. For instance, most models focus primarily on vaccination without considering the full potential of combining quarantine measures and public awareness campaigns. Moreover, the role of socio-economic factors and varying healthcare infrastructure in different regions has not been adequately explored [22, 23]. Addressing these gaps is essential for developing a comprehensive approach that can be effectively tailored to different demographic and regional contexts.

Given the importance of preventing measles outbreaks, multiple policies should be adopted, including widespread vaccination, quarantine for exposed individuals, and seeking medical attention at the onset of symptoms. It is also critical to develop public health education programs

that enhance community awareness and engagement in vaccination drives. Recent studies have emphasized the need for robust health communication strategies to improve vaccine uptake and adherence to quarantine protocols during outbreaks [22, 24].

This article proposes a comprehensive mathematical model to assess the effectiveness of these measures in controlling measles. The model includes five components: susceptible, exposed, infected with severe complications, infected with mild complications, and recovered. By integrating vaccination coverage data with quarantine effectiveness and public health education impact, the model aims to provide a holistic view of measles control. The goal is to determine the optimal vaccination coverage to prevent the spread of measles effectively and to identify the most impactful strategies for public health interventions [25, 26]. The potential implications of this research are far-reaching. By developing a more comprehensive understanding of measles transmission dynamics and control measures, policymakers and public health officials can make more informed decisions that enhance the effectiveness of measles prevention and control programs. The model can also be adapted to study other infectious diseases, thereby broadening its applicability and utility. Additionally, the insights gained from this research can inform the development of integrated public health strategies that combine vaccination, quarantine, and education in a synergistic manner, ultimately leading to more sustainable and impactful health outcomes [27–29].

2. MODEL FORMULATION

We present a continuous SEI_HI_LHR model to describe the interactions within a population where measles is present. The population is divided into six compartments: Susceptible (S), Exposed (E), Infected with high complications (I_H), Infected with low complications (I_L), Hospitalized (H) and Recovered (R). The total population at time t is represented by $N = S+E+I_H+I_L+H+R$. The proposed model is graphically depicted in Figure (1).

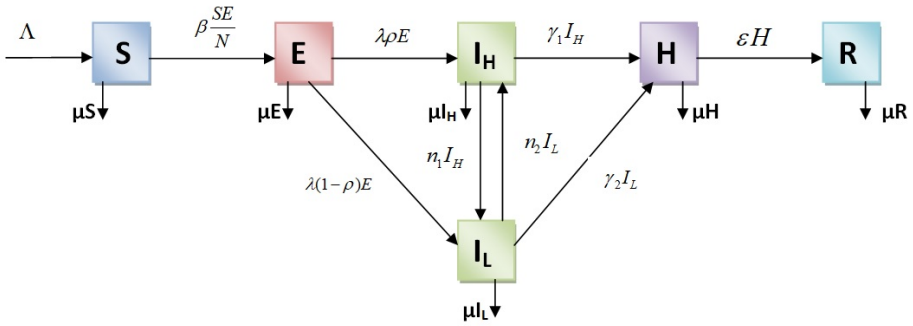

FIGURE 1. Model description.

We conduct an analysis of a system made up of five non-linear differential equations:

$$
\begin{cases}
\dfrac{dS(t)}{dt} = \Lambda - \beta\dfrac{E(t)S(t)}{N} - \mu_1 S(t), \\
\dfrac{dE(t)}{dt} = \beta\dfrac{E(t)S(t)}{N} - (\lambda+\mu_2)E(t), \\
\dfrac{dI_H(t)}{dt} = \lambda\rho E(t) - (n_1+\gamma_1+\mu_3+\theta)I_H(t) + n_2 I_L(t,) \\
\dfrac{dI_L(t)}{dt} = \lambda(1-\rho)E(t) - (n_2+\gamma_2+\mu_4)I_L(t) + n_1 I_H(t), \\
\frac{dH(t)}{dt} = \gamma_1 I_H(t) + \gamma_2 I_L(t) n_1 - (\varepsilon+\mu_5)H(t), \\
\dfrac{dR(t)}{dt} = \varepsilon H(t) - \mu_6 R(t).
\end{cases}
\tag{2.1}
$$

Taking into account the initial conditions provided

$$
S(0) \geq 0\ ,\ E(0) \geq 0\ ,\ I_H(0) \geq 0\ ,\ I_L(0) \geq 0\ ,\ H(0) \geq 0 \quad \textit{and} \quad R(0) \geq 0 \tag{2.2}
$$

Table (1) contains further details about the parameters of our model.

Parameter	Description
Λ	Indicates the rate of new births in the sensitive human population.
β	Indicates the transmission coefficient from susceptible individuals to exposed cases.
λ	Represents the transmission rate from exposed cases to cases presenting mild symptoms or cases presenting severe symptoms.
θ	Represents the mortality rate due to the disease.
n1	Represents the transmission rate from mildly infected individuals to severely infected individuals.
n2	Represents the transmission rate from severely infected individuals to mildly infected individuals.
γ_1**et**γ_2	Represent the transmission coefficients from infected individuals with mild symptoms and severe symptoms to hospitalized cases.
ε	Specifies the transmission coefficient for the shift from hospitalized cases to recovered cases.
μ	Indicates the natural mortality rate in all compartments.

TABLE 1. Description of the parameters of the measles model .

2.1. Model Basic Properties.

2.1.1. *Invariant Region.*

Lemma 1. *The valid region* Ω *specified by:*

$$\Omega = \left\{ (S,E,I_H,I_L,H,R) \in \mathbb{R}^6_+ : 0 \leq S+E+I_H+I_L+H+R \leq \frac{\Lambda}{\mu} \right\}.$$

Given the conditions $E(0) \geq 0$, $S(0) \geq 0$, $I_H(0) \geq 0$, $I_L(0) \geq 0$, $H(0) \geq 0$ *and* $R(0) \geq 0$

Proof. by définition

$$N = S+E+I_H+I_L+H+R, \tag{2.3}$$

hence

$$\frac{dN}{dt} = \Lambda - \mu N - \theta I_H, \tag{2.4}$$

$$\frac{dN}{dt} = \Lambda - \mu N - \theta I_H \leq \Lambda - \mu N. \tag{2.5}$$

Implies that

$$\frac{dN}{dt} \leq \Lambda - \mu N. \tag{2.6}$$

It follows that

$$N(t) \leq e^{-\mu t} N(0) + \frac{\Lambda}{\mu}(1 - e^{-\mu t}). \tag{2.7}$$

Considering that $N(0)$ denotes the initial total population, thus,

$$\lim_{t \to +\infty} \sup N(t) \leq \frac{\Lambda}{\mu}. \tag{2.8}$$

This implies that the region Ω serves as a non-negativity invariant set for the system (2.1).

$$N(t) \leq \frac{\Lambda}{\mu}. \tag{2.9}$$

□

2.1.2. *Non-negativity of solutions.*

Theorem 2. *If the initial values are such that $E(0) \geq 0$, $S(0) \geq 0$, $I_H(0) \geq 0$, $I_L(0) \geq 0$, $H(0) \geq 0$, and $R(0) \geq 0$ and given the initial time $t \geq 0$, then the solutions of the system will remain positive for all $t \geq 0$. This ensures that the model maintains non-negative values for all compartments over time, preserving the physical meaning of the quantities involved.*

Proof. The initial equation of system (2.1) suggests that

$$\frac{dS(t)}{dt} = \Lambda - A(t)S(t). \tag{2.10}$$

Where $A(t) = \beta \frac{E(t)}{N} + \mu_1$.

we apply a multiplication to equation (2.10) by $\exp\left(\int_0^t A(s)ds\right)$, we find

$$\exp\left(\int_0^t A(s)ds\right).\frac{dS(t)}{dt} + \exp\left(\int_0^t A(s)ds\right).A(t).S(t) = \exp\left(\int_0^t A(s)ds\right)\Lambda. \tag{2.11}$$

Implies that

$$\frac{d}{dt}\left(S(t).\exp\left(\int_0^t A(s)ds\right)\right) = \Lambda.\exp\left(\int_0^t A(s)ds\right). \tag{2.12}$$

Integrating with respect to s from 0 to t, we obtain

$$S(t).\exp\left(\int_0^t A(s)ds\right) = \Lambda.\int_0^t \exp\left(\int_0^\omega A(s)ds\right)d\omega + S(0). \tag{2.13}$$

By multiplying equation (2.13) by $\exp\left(-\int_0^t A(s)ds\right)$, we obtain:

(2.14)

$$S(t) = \Lambda.\exp\left(-\int_0^t A(s)ds\right)\int_0^t \exp\left(\int_0^\omega A(s)ds\right)d\omega + \exp\left(-\int_0^t A(s)ds\right).S(0) \geq 0.$$

Thus, the solution $S(t)$ retains its positivity.

In a similar manner, from the remaining equations of system (2.1), we determine that $E(t) \geq 0$, $I_H(t) \geq 0$, $I_L(t) \geq 0$, $H(t) \geq 0$, and $R(t) \geq 0$. □

The initial four equations in system (2.1) do not depend on the variables H and R. As a result, the behavior of the system of equations (2.1) is analogous to the behavior of the following system of equations:

$$
\begin{cases}
\dfrac{dS(t)}{dt} = \Lambda - \beta \dfrac{S(t)E(t)}{N} - \mu_1 S(t), \\
\dfrac{dE(t)}{dt} = \beta \dfrac{S(t)E(t)}{N} - (\lambda + \mu_2)E(t), \\
\dfrac{dI_H(t)}{dt} = \lambda \rho E(t) - (n_1 + \gamma_1 + \mu_3 + \theta)I_H(t) + n_2 I_L(t), \\
\dfrac{dI_L(t)}{dt} = (1-\rho)\lambda E(t) - (n_2 + \gamma_2 + \mu_4)I_L(t) + n_1 I_H(t).
\end{cases} \tag{2.15}
$$

2.2. The Equilibrium Points. System (2.15) encompasses the following two equilibrium points, which are critical for understanding the behavior of the system under different conditions. These equilibrium points help to analyze the stability and dynamics of the system, providing insight into its long-term behavior and potential steady states.

2.2.1. ***Disease-free equilibrium point.*** The measles disease-free equilibrium $E^0_{eq}(\frac{\Lambda}{\mu}, 0, 0, 0)$ is achieved in the absence of virus ($I_L = I_H = E = 0$).

2.2.2. ***Endemic equilibrium point.*** The measles disease present equilibrium $E^*_{eq}(S^*, E^*, I^*_H, I^*_L)$ is archieved when the deasese exists ($E \neq 0, I^*_L \neq 0$ *and* $I^*_L \neq 0$).

where

$$S^* = \frac{N}{\beta}(\lambda + \mu_2), \tag{2.16}$$

$$E^* = \frac{N\mu_1}{\beta}(R_0 - 1), \tag{2.17}$$

$$I^*_H(t) = \frac{\lambda\left(\alpha_2\rho + n_2\lambda(1-\rho)\right)\mu_1 N}{\beta\left(\alpha_1\alpha_2 - n_1 n_2\right)}(R_0 - 1), \tag{2.18}$$

and

$$I^*_L(t) = \frac{\lambda\left(n_1\rho + \alpha_2\lambda(1-\rho)\right)\mu_1 N}{\beta\left(\alpha_1\alpha_2 - n_1 n_2\right)}(R_0 - 1). \tag{2.19}$$

With

$$
\begin{cases}
\alpha_1 = n_1 + \gamma_1 + \mu_3 + \theta \\
\alpha_2 = n_2 + \gamma_2 + \mu_4
\end{cases}, \tag{2.20}
$$

$$R_0 = \frac{\beta\Lambda}{\mu_1 N(\lambda + \mu_2)}. \tag{2.21}$$

The basic reproduction number, denoted as R_0, measures the average number of new infections produced by one infected individual in a population where all members are susceptible.

2.3. Analysis of Model Parameter Stability and Sensitivity. In this segment of our research, we delve into examining the system's stability at its equilibrium states, addressing both conditions: when the disease is present and when it is absent.

2.3.1. ***analysis of local stability***. We explore the local stability characteristics at the equilibrium points E_{eq}^0 and E_{eq}^*. This detailed analysis involves studying the system's behavior near these equilibrium points to determine whether small disturbances will diminish over time, returning the system to equilibrium, or whether they will amplify, leading to instability. Understanding these stability properties is essential for predicting the system's response to minor perturbations and ensuring the robustness of the equilibrium states.

2.3.1.1. Point of equilibrium without disease.

Theorem 3. *The measles disease-free equilibrium $E_{eq}^0(\frac{\Lambda}{\mu},0,0,0)$ of the system (2.15) is asymptotically stable if $R_0 \prec 1$ and instable if $R_0 \succ 1$.*

Proof. The Jacobian matrix at E_{eq}^0 is given by:

$$J\left(E_{eq}^0\right) = \begin{pmatrix} -\mu & \frac{-\beta\Lambda}{\mu N} & 0 & 0 \\ 0 & \frac{\beta\Lambda}{\mu N} - (\lambda+\mu) & 0 & 0 \\ 0 & \lambda\rho & -(n_1+\gamma_1+\mu+\theta) & n_2 \\ 0 & \lambda(1-\rho) & n_1 & -(n_2+\gamma_2+\mu) \end{pmatrix}. \tag{2.22}$$

The characteristic equation for this matrix can be written as $\det\left(J\left(E_{eq}^0\right) - \xi I_4\right) = 0$, with I_4 being a 4*x*4 identity matrix.

$$\det\left(J\left(E_{eq}^0\right) - \xi I_4\right) = 0, \tag{2.23}$$

$$-(\mu+\xi)\left[\left(\frac{\beta\Lambda}{\mu N} - \lambda - \mu - \xi\right)\left((n_1+\gamma_1+\mu+\theta+\xi)(n_2+\gamma_2+\mu+\xi) - n_1 n_2\right)\right] = 0. \tag{2.24}$$

Thus, the eigenvalues derived from the characteristic equation of matrix $J\left(E_{eq}^0\right)$ are as follows:

$$\begin{cases} \xi_1 = -\mu, \\ \xi_2 = (\lambda+\mu)(R_0-1), \\ \xi_3 = \frac{-(k_1+k_2)-\sqrt{(k_1-k_2)^2+4n_1n_2}}{2}, \\ \xi_4 = \frac{-(k_1+k_2)+\sqrt{(k_1-k_2)^2+4n_1n_2}}{2}. \end{cases} \tag{2.25}$$

Where

$$\begin{cases} k_1 = n_1+\gamma_1+\mu+\theta, \\ k_2 = n_2+\gamma_2+\mu. \end{cases} \tag{2.26}$$

Hence, if condition $R_0 \prec 1$ is met, it follows that all the eigenvalues of the characteristic equation $J\left(E^0_{eq}\right)$ are negative real numbers.

Therefore, it can be deduced that the system (2.15) at the disease-free equilibrium point $E^0_{eq}(\frac{\Lambda}{\mu},0,0,0)$ is asymptotically stable under condition $R_0 \prec 1$, but becomes unstable when condition $R_0 \succ 1$ is present. □

2.3.1.2. Equilibrium point in the presence of disease.

Theorem 4. *Equilibrium points with disease $E^*_{eq}(S^*,E^*,I^*_H,I^*_L)$ of system (2.15) is asymptotically stable if $R_0 \succ 1$ and is unstable if $R_0 \prec 1$.*

Proof. The Jacobian matrix at E^*_{eq} is given by:

$$J\left(E^*_{eq}\right) = \begin{pmatrix} -\mu R_0 & -(\lambda+\mu) & 0 & 0 \\ \mu(R_0-1) & 0 & 0 & 0 \\ 0 & \lambda\rho & -k_1 & n_2 \\ 0 & \lambda(1-\rho) & n_1 & -k_2 \end{pmatrix}. \tag{2.27}$$

It is observed that the characteristic equation $\varphi(\zeta)$ is associated with matrix $J\left(E^*_{eq}\right)$.

$$\varphi(\zeta) = \xi^4 + a_1\xi^3 + a_2\xi^2 + a_3\xi + a_4. \tag{2.28}$$

where,

$$\begin{aligned} a_1 &= \mu R_0 + k_1 + k_2, \\ a_2 &= \mu R_0(k_1+k_2) + k_1k_2 - n_1n_2 - \mu(\lambda+\mu)(R_0-1), \end{aligned} \tag{2.29}$$

$$a_3 = \mu R_0 (k_1 k_2 - n_1 n_2) - \mu (\lambda + \mu)(R_0 - 1)(k_1 + k_2),$$
$$a_4 = -(k_1 k_2 - n_1 n_2)\mu (\lambda + \mu)(R_0 - 1).$$

Based on the Routh-Hurwitz criterion [30], system (2.15) achieves local asymptotic stability under the condition specified by $a_1 \succ 0$, $a_2 \succ 0$, $a_3 \succ 0$, $a_4 \succ 0$ and $(a_1 a_2 - a_3) a_3 \succ {a_1}^2 a_4$. Therefore, for system (2.15), the current equilibrium point $E^*_{eq}(S^*, E^*, I^*_H, I^*_L)$ is considered locally asymptotically stable when condition $R_0 \succ 1$ is satisfied. □

2.3.2. *Global Stability*.

2.3.2.1. Overall stability in the absence of disease. To establish the global asymptotic stability of system (2.13), we utilize Lyapunov function theory for both the measles disease-free equilibrium and the measles endemic equilibrium. We begin by demonstrating the global stability of the measles disease-free equilibrium, referred to as E^0_{eq}. This involves constructing a suitable Lyapunov function and proving that it satisfies the necessary conditions to ensure stability for the disease-free state.

Theorem 5. *The MEASLES disease-free equilibrium E^0_{eq} is globally asymptotically stable if condition $R_0 \leq 1$ is met, and it is unstable under any other circumstances.*

Proof. Let's consider the following Lyapunov function for our analysis:

$$V : \Gamma \to \mathbb{R}$$
$$V(S, E, I_H, I_L) = E \quad ,$$

where $\Gamma = \{(S, E, I_H, I_L) \in \Gamma / S \succ 0, E \succ 0, I_H \succ 0, I_L \succ 0\}$ then the derivative of the Lyapunov function is given by :

$$\frac{dV}{dt} = \frac{dE}{dt} = (\frac{\beta \Lambda}{\mu_1 N} - (\alpha + \mu_2))E,$$
$$\frac{dV}{dt} = (\alpha + \mu_2)(R_0 - 1)E.$$

So, $\frac{dV}{dt} \leq 0$ if $R_0 \leq 1$ also $\frac{dV}{dt} = 0$ if and only if $E = 0$ then, E^0_{eq} is globally asymtitically. □

2.3.2.2. Global stability in the presence of disease. The conclusive outcome regarding the global stability of E^*_{eq} in this section can be summarized as follows:

Theorem 6. *The equilibrium point with disease E^*_{eq} of system (2.15) is globally asymptotically stable if the basic reproduction number R_0 is greater than 1.*

Proof. We examine the following Lyapunov function:

$$V : \Gamma \to \mathbb{R}$$
$$V(E,S) = E - E^* \ln\left(\frac{E}{E^*}\right) + S - S^* \ln\left(\frac{S}{S^*}\right), \tag{2.30}$$

where $\Gamma = \{(S,E,I_H,I_L) \in \Gamma / S \succ 0, E \succ 0\}$ then the derivative of the Lyapunov function is given by:

$$\frac{dV(S,E)}{dt} = (-\frac{\Lambda(S-S^*)}{SS^*} - \frac{\beta}{N}(E-E^*))(S-S^*) + \frac{\beta}{N}(S-S^*)(E-E^*), \tag{2.31}$$

then

$$\frac{dV(S,E)}{dt} = -\frac{\Lambda(S-S^*)^2}{SS^*} \leq 0, \tag{2.32}$$

furthermore, we obtain

$$\frac{dV(P,M)}{dt} = 0 \quad \Leftrightarrow \quad S = S^*. \tag{2.33}$$

Hence, using LaSalle's invariance principle [21], it follows that the equilibrium point E^*_{eq} for measles is globally asymptotically stable within the region Γ. □

2.3.3. ***Sensitivity Analysis of*** R_0. Sensitivity analysis is widely applied to evaluate a model's resilience against variations in its parameters. This process is instrumental in pinpointing which parameters exert a substantial effect on the basic reproduction number, R_0, given that data collection and parameter assumptions are frequently prone to errors.

Employing the methodology outlined by Chitnis et al [20], we compute the normalized forward sensitivity indices for R_0. Let

$$\Upsilon^{R_0}_n = \frac{\partial R_0}{\partial n} * \frac{n}{R_0}. \tag{2.34}$$

Indicating the sensitivity index of R_0 in relation to the parameter n, we obtain

$$R_0 = \frac{\Lambda\beta}{\mu N(\lambda+\mu)}, \tag{2.35}$$

$$\Upsilon^{R_0}_\beta = 1, \tag{2.36}$$

$$\Upsilon_{\mu}^{R_0} = -\frac{\mu}{\lambda+\mu} - 1, \tag{2.37}$$

$$\Upsilon_{\lambda}^{R_0} = -\frac{\lambda}{\lambda+\mu}. \tag{2.38}$$

The sensitivity values are as follows:

Υ_{β}	1
Υ_{μ}	-0.25
Υ_{λ}	-1.7

From the above, it's clear that the basic reproduction number, R_0, is highly responsive to variations in β. Specifically, a rise in β directly elevates R_0 by the same ratio, whereas a decline in β reduces R_0 proportionally. Conversely, μ and λ are inversely related to R_0, meaning that an increase in either will result in a reduction of R_0.

3. SIMULATION

In this section, we present several numerical solutions for Model (Figure 1) using the following initial values $S+E+I_H+I_L+H+R = 305000$.

The parameter values (Table 2) have been chosen based on hypothetical scenarios due to the lack of available real-world data. This approach allows us to construct and analyze the model effectively in the absence of empirical data, ensuring that our theoretical framework can still provide valuable insights. By using hypothetical data, we can explore a range of possible outcomes and dynamics within the model, which can later be validated against real data once it becomes available. This method also helps in identifying potential limitations and areas for further research.

Parameters	Values
$(\Lambda, \mu, \beta, \varepsilon, \gamma_1, \gamma_2, n_1, n_2, \rho)$	(800,0.002,0.4,0.6,0.28,0.28,0.2,0.4,0.72)

TABLE 2. Parameters for the model.

3.1. Disease-free equilibrium. In our study, we applied and presented several numerical simulations for the system defined in equations (2.1), demonstrating our results with specific parameter estimates and varying initial conditions for each state variable. Our simulations indicate

that the disease-free equilibrium (measles) has an R_0 value of 0.050, which is less than 1. According to theorem (3), this suggests that the measles disease-free equilibrium E_0 of system (2.1) is globally asymptotically stable within the defined domain Ω, as depicted in figures (2,3,...,7).

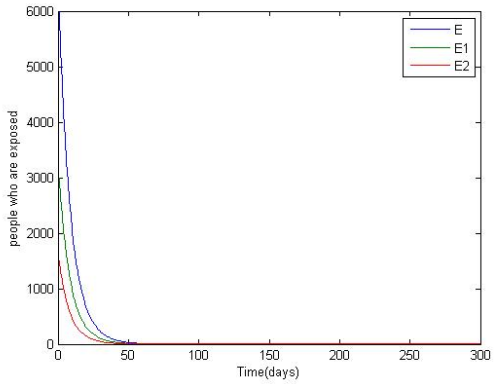

FIGURE 2. Exposed

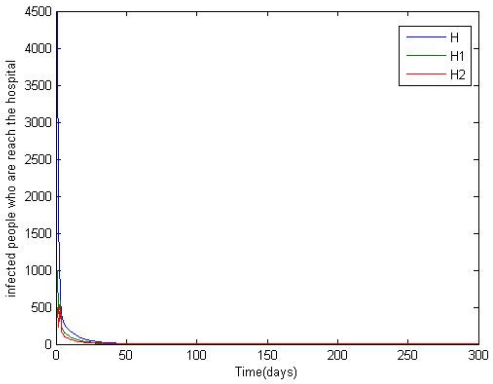

FIGURE 3. Hospitalized

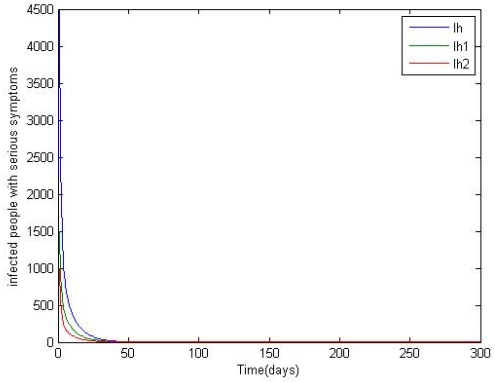

FIGURE 4. Infected with severe symptoms

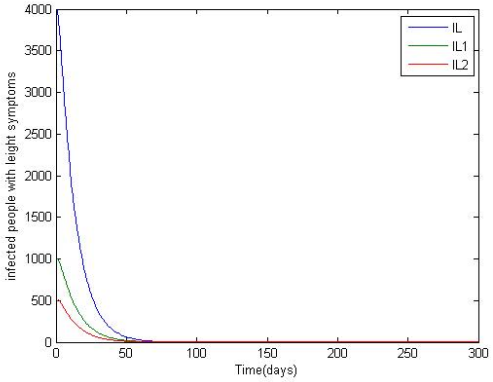

FIGURE 5. Infected with mild symptoms

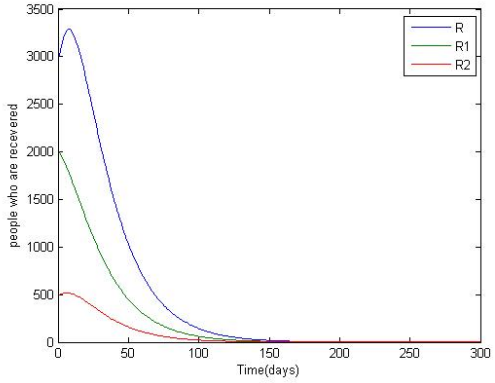

FIGURE 6. Recovered

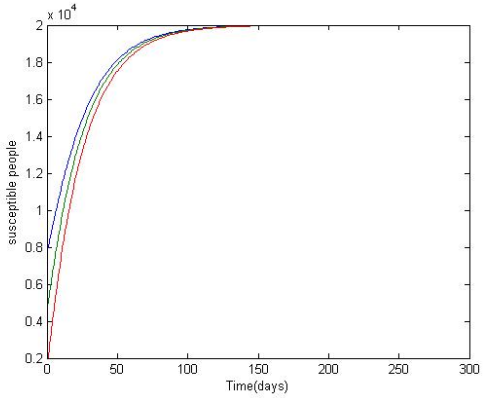

FIGURE 7. Susceptible

Based on this information, we derived the following observations:

Comments:

(1) The number of susceptible individuals increases steadily over time and eventually approaches the population value of $S_0 = 2.00e+04$ (refer to Figure 7 for more details).
(2) The number of exposed individuals declines gradually and converges towards zero (as shown in Figure 2).
(3) The count of individuals infected with severe symptoms, as well as those who are virus carriers, tends towards zero (see Figure 4 for a visual representation).
(4) The number of individuals infected with mild symptoms and virus carriers similarly approaches zero (refer to Figure 5 for this trend).
(5) The number of hospitalized cases is on a downward trajectory and is nearing zero (see Figure 3 for further details).
(6) The count of recovered cases also decreases over time and approaches zero (as illustrated in Figure 6).

Consequently, when the basic reproduction number $R_0 \leq 1$, model (Figure 1) exhibits global asymptotic stability.

3.2. Point of equilibrium with disease: Moreover, considering the parameters and varying initial values for each state variable, we observe an equilibrium point with measles E_{eq} and $R_0 = 2.1858 > 1$. This indicates that system (2.1) is globally asymptotically stable within the domain Ω (see figures (8,9,...,13)).

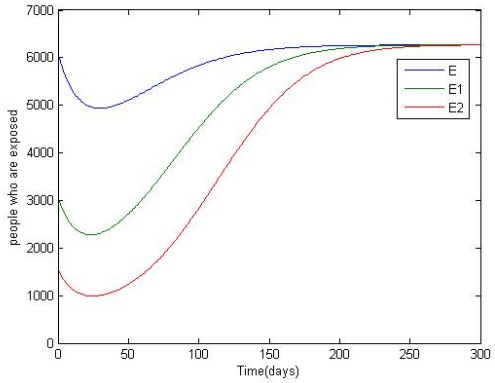

FIGURE 8. Exposed

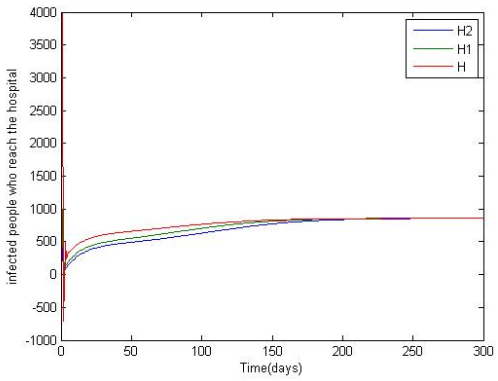

FIGURE 9. Hospitalized

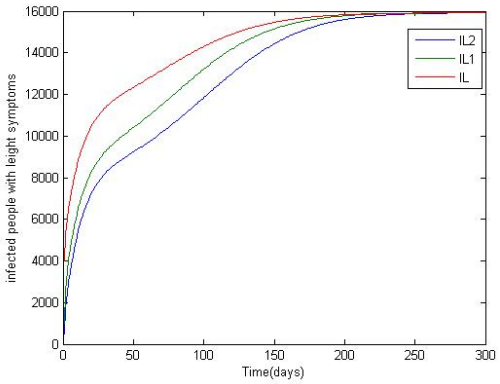

FIGURE 10. Infected with mild symptoms

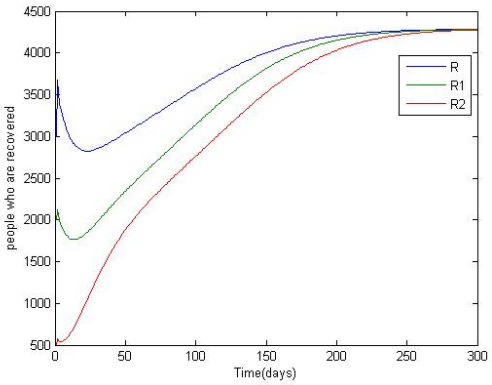

FIGURE 11. Recovered

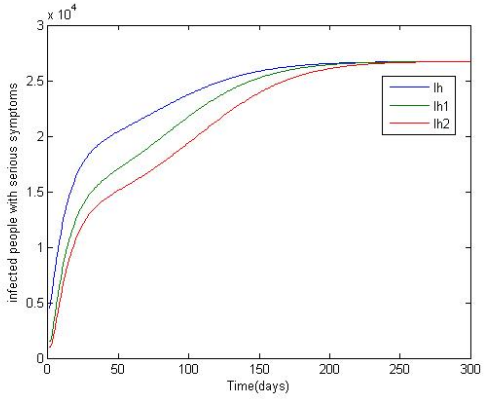

FIGURE 12. Infected with severe symptoms

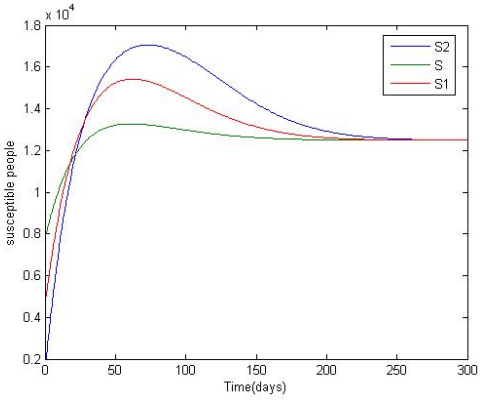

FIGURE 13. Susceptible

(1) The number of susceptible individuals initially increases, followed by a slight decrease, eventually approaching the value $S^* = 1.2e+04$ (refer to Figure 13 for a detailed visualization).

(2) The count of exposed cases rises over time and eventually stabilizes at $E^* = 6000$ (see Figure 8 for more information).

(3) The number of individuals with severe symptoms and virus carriers experiences a slight decrease, approaching a value of $I_H^* = 2.7e+04$ (refer to Figure 12).

(4) The count of individuals infected with mild symptoms and virus carriers also decreases gradually, moving towards $I_L^* = 1.6e+04$ (see Figure 10 for further details).

(5) The number of hospitalized cases shows a declining trend and moves towards convergence (this pattern is illustrated in Figure 9).

(6) The count of individuals who have recovered from the illness shows a downward trend and eventually stabilizes at approximately $R^* = 4300$. This pattern of recovery rate is clearly depicted in Figure 11, indicating that the system reaches a steady state for the number of recovered cases over time.

- Thus, the trajectories of the solution curves trend towards the equilibrium point $E^*_{eq}(S^*, E^*, I^*, Q^*, R^*)$ when $R_0 > 1$. Therefore, this indicates that model (2.1) is globally asymptotically stable, meaning that over time, the system will settle into a stable state where the disease persists in the population at a constant level.

4. Conclusion

In our article, we've constructed a continuous mathematical model to capture the dynamics of measles infections. We've identified the basic reproduction number R_0 as $\frac{\beta\Lambda}{\mu_1 N(\lambda+\mu_2)}$, essential for grasping the outbreak's mechanics. Additionally, we carried out a sensitivity analysis on the parameters significantly affecting R_0. By applying stability analysis to nonlinear systems, we scrutinized the measles mathematical model, investigating its local and global stability phases. We elucidated that the disease-free equilibrium point, E^0_{eq}, achieves local stability when R_0 is greater than 1. In contrast, when R_0 is less than or equal to 1, the disease present equilibrium points, E^*_{eq}, are locally asymptotically stable. We've established the global asymptotic stability of E^0_{eq} and E^*_{eq} under their respective R_0 conditions using Lyapunov functions, enhancing our understanding of disease control and prevention dynamics.

Conflict of Interests

The authors declare that there is no conflict of interests.

References

[1] P.L. Panum, Observations Made During the Epidemic of Measles on the Faroe Islands in the Year 1846, in: The Challenge of Epidemiology: Issues and Selected Readings, Pan American Health Organization, New York, pp. 37–41, 1988.

[2] CDC, Vaccines and Immunizations-Measles Epidemiology and Prevention of Vaccine-Preventable Diseases, Centers for Disease Control and Prevention, 2016.

[3] S.R.B. Shrivastava, P.S. Shrivastava, J. Ramasamy, Enormous Need to Improve the Global Measles Vaccination Coverage: World Health Organization, MAMC J. Med. Sci. 2 (2016), 109-110.

[4] J. Zhang, B. Feng, The Geometric Theory and Bifurcation Problem of Ordinary Differential Equation, Peking University Press, Beijing, 1987.

[5] G.Q. Zhang, Q.B. Sun, L. Wang, Noise-Induced Enhancement of Network Reciprocity in Social Dilemmas, Chaos Solitons Fractals 51 (2013), 31–35. https://doi.org/10.1016/j.chaos.2013.03.003.

[6] H.F. Zhang, Z. Yang, Z.X. Wu, et al. Braess's Paradox in Epidemic Game: Better Condition Results in Less Payoff, Sci. Rep. 3 (2013), 3292. https://doi.org/10.1038/srep03292.

[7] H. Zhang, J. Zhang, C. Zhou, et al. Hub Nodes Inhibit the Outbreak of Epidemic under Voluntary Vaccination, New J. Phys. 12 (2010), 023015. https://doi.org/10.1088/1367-2630/12/2/023015.

[8] H.F. Zhang, Z.X. Wu, M. Tang, et al. Effects of Behavioral Response and Vaccination Policy on Epidemic Spreading - An Approach Based on Evolutionary-Game Dynamics, Sci. Rep. 4 (2014), 5666. https://doi.org/10.1038/srep05666.

[9] C. Xia, Z. Wang, J. Sanz, et al. Effects of Delayed Recovery and Nonuniform Transmission on the Spreading of Diseases in Complex Networks, Physica A: Stat. Mech. Appl. 392 (2013), 1577–1585. https://doi.org/10.1016/j.physa.2012.11.043.

[10] M.J. Keeling, P. Rohani, Modeling Infectious Diseases in Humans and Animals, Princeton University Press, 2011.

[11] P. Van Den Driessche, J. Watmough, Reproduction Numbers and Sub-Threshold Endemic Equilibria for Compartmental Models of Disease Transmission, Math. Biosci. 180 (2002), 29–48. https://doi.org/10.1016/S0025-5564(02)00108-6.

[12] O. Diekmann, J.A.P. Heesterbeek, Mathematical Epidemiology of Infectious Diseases: Model Building, Analysis and Interpretation, John Wiley & Sons, 2000.

[13] M.S. Bartlett, Measles Periodicity and Community Size, J. R. Stat. Soc. Ser. A 120 (1957), 48-70. https://doi.org/10.2307/2342553.

[14] B.M. Bolker, B.T. Grenfell, Impact of Vaccination on the Spatial Correlation and Persistence of Measles Dynamics, Proc. Nat. Acad. Sci. 93 (1996), 12648–12653. https://doi.org/10.1073/pnas.93.22.12648.

[15] D.J.D. Earn, P. Rohani, B.M. Bolker, et al. A Simple Model for Complex Dynamical Transitions in Epidemics, Science 287 (2000), 667–670. https://doi.org/10.1126/science.287.5453.667.

[16] M.J. Ferrari, R.F. Grais, N. Bharti, et al. The Dynamics of Measles in Sub-Saharan Africa, Nature 451 (2008), 679–684. https://doi.org/10.1038/nature06509.

[17] M. Baroudi, H. Gourram, A. Labzai, et al. Mathematical Modeling and Monkeypox's Optimal Control Strategy, Commun. Math. Biol. Neurosci. 2023 (2023), 110. https://doi.org/10.28919/cmbn/8198.

[18] H. Gourram, M. Baroudi, A. Labzai, et al. Mathematical Modeling and Optimal Control Strategy for the Influenza (H5N1), Commun. Math. Biol. Neurosci. 2023 (2023), 113. https://doi.org/10.28919/cmbn/8199.

[19] A. Labzai, M. Baroudi, M. Belam, et al. Stability Analysis of an Order Fractional of a New Corona Virus Disease (COVID-19) Model, Commun. Math. Biol. Neurosci. 2023 (2023), 77. https://doi.org/10.28919/cmbn/8064.

[20] A.S. Belenky, D.C. King, A Mathematical Model for Estimating the Potential Margin of State Undecided Voters for a Candidate in a US Federal Election, Mathematical and Computer Modelling 45 (2007), 585–593. https://doi.org/10.1016/j.mcm.2006.07.007.

[21] W. Mei, F. Bullo, LaSalle Invariance Principle for Discrete-Time Dynamical Systems: A Concise and Self-Contained Tutorial, arXiv:1710.03710 [math.DS] (2017). https://doi.org/10.48550/arXiv.1710.03710.

[22] M.G. Roberts, M.I. Tobias, Predicting and Preventing Measles Epidemics in New Zealand: Application of a Mathematical Model, Epidemiol. Infect. 124 (2000), 279–287. https://doi.org/10.1017/S0950268899003556.

[23] H.T. Alemneh, A.M. Belay, Modelling, Analysis, and Simulation of Measles Disease Transmission Dynamics, Discr. Dyn. Nat. Soc. 2023 (2023), 9353540. https://doi.org/10.1155/2023/9353540.

[24] E.K. Szusz, L.P. Garrison, C.T. Bauch, A Review of Data Needed to Parameterize a Dynamic Model of Measles in Developing Countries, BMC Res. Notes 3 (2010), 75. https://doi.org/10.1186/1756-0500-3-75.

[25] F.T. Cutts, E. Dansereau, M.J. Ferrari, et al. Using Models to Shape Measles Control and Elimination Strategies in Low- and Middle-Income Countries: A Review of Recent Applications, Vaccine 38 (2020), 979–992. https://doi.org/10.1016/j.vaccine.2019.11.020.

[26] O.M. Tessa, Mathematical Model for Control of Measles by Vaccination, in: Proceedings of Mali Symposium on Applied Sciences, 2006.

[27] D.N. Durrheim, N.S. Crowcroft, P.M. Strebel, Measles – The Epidemiology of Elimination, Vaccine 32 (2014), 6880–6883. https://doi.org/10.1016/j.vaccine.2014.10.061.

[28] P. Bosetti, P. Poletti, M. Stella, et al. Heterogeneity in Social and Epidemiological Factors Determines the Risk of Measles Outbreaks, Proc. Nat. Acad. Sci. 117 (2020), 30118–30125. https://doi.org/10.1073/pnas.1920986117.

[29] L.E. Markowitz, W.A. Orenstein, Measles Vaccines, Pediatr. Clin. North Amer. 37 (1990), 603–625. https://doi.org/10.1016/S0031-3955(16)36907-3.

[30] E.X. DeJesus, C. Kaufman, Routh-Hurwitz Criterion in the Examination of Eigenvalues of a System of Nonlinear Ordinary Differential Equations, Phys. Rev. A 35 (1987), 5288–5290. https://doi.org/10.1103/PhysRevA.35.5288.

[31] M. Baroudi, I. Smouni, H. Gourram, A. Labzai, M. Belam, Optimizing Control Strategies for Monkeypox through Mathematical Modeling, Partial Differ. Equ. Appl. Math. 12 (2024), 100996. https://doi.org/10.1016/j.padiff.2024.100996.

[32] I. Smouni, M. Baroudi, M. Alia, A. Elmansouri, A. Labzai, M. Belam, Spatiotemporal Stability Analysis of Soil-Borne Disease Dynamics in Tomato Plants, Model. Earth Syst. Environ. 11 (2025), 105. https://doi.org/10.1007/s40808-024-02187-w.

[33] M. Baroudi, H. Gourram, A. Labzai, et al. Mathematical Modeling and Monkeypox's Optimal Control Strategy, Commun. Math. Biol. Neurosci. 2023 (2023), 110. https://doi.org/10.28919/cmbn/8198.